

All Electron Full Potential APW+*lo* calculation using Exciting-Plus and SIRIUS library

Long Zhang,^{1,2,3} Anton Kozhevnikov,⁴ Thomas Schulthess,⁴ S. B. Trickey,^{1,2,3} and Hai-Ping Cheng^{1,2,3, a)}

¹⁾*Department of Physics, University of Florida, Gainesville, FL 32611, USA*

²⁾*Quantum Theory Project, University of Florida, Gainesville, FL 32611, USA*

³⁾*Center for Molecular Magnetic Quantum Materials, University of Florida, Gainesville, FL 32611, USA*

⁴⁾*Swiss National Supercomputing Centre, Zurich, Switzerland*

(Dated: 30 Apr. 2021)

We report the interfacing of the Exciting-Plus (“EP”) FLAPW DFT code with the SIRIUS multi-functional DFT library. Use of the SIRIUS library enhances EP with additional task parallelism in ground state DFT calculations. Without significant change in the EP source code, the additional eigensystem solver method from the SIRIUS library can be exploited for performance gains in diagonalizing the Kohn-Sham Hamiltonian. We benchmark the interfaced code against the original EP using small bulk systems, and then demonstrate performance on much larger molecular magnet systems that are well beyond the capability of the original EP code.

^{a)}Electronic mail: hping@ufl.edu

I. INTRODUCTION

Molecular magnetism is a very active interdisciplinary research area that has significant implications for computational investigations. Motivated in no small measure by the promise of high impact on quantum computing^{1,2}, molecular magnetism deals with design, synthesis, and physical and chemical characterization of both single molecule magnets (SMMs)^{3,4} and condensed aggregates thereof. Predictive and interpretive first principles calculations are highly relevant both with respect to experimental progress and for formulation and parameterization of models of the molecular spin systems. We begin therefore with a brief overview of the physical problem class, then turn to attendant computational challenges and our progress in meeting them.

A. Motivation from physical systems

Molecular magnetism covers a large range of dimensionality, from isolated SMMs^{5,6} and 1D chain magnets^{7,8} through 2D molecular layers⁹ to 3D polymers and metal organic framework^{10,11} materials that exhibit collective ordering of magnetic moments.

Research activity, both theoretical and experimental, on molecule-based materials has grown in recent decades with focus on (1) low dimensional materials (motivated by their potential application in high-density magnetic storage and nano-scale devices)^{12,13} and (2) so-called functional materials^{5,12,14,15} (because of their strong response to changing external conditions). Because molecular magnets have well-localized magnetic moments, they are a nearly perfect playground for investigation of intriguing phenomena and testing models. Unlike bulk magnetic materials, their quantum size effects suggest applications beyond conventional high-density information storage. Such applications include spintronics and qubits for quantum computing.

The molecules involved are large and rather complicated. An example category is Mn₁₂ complexes¹⁶. Their investigation dates to synthesis by Weinland and Fischer in 1921¹⁷. The crystal structure was not determined until 1980¹⁸. That particular Mn₁₂ molecule was built from four Mn₄₊ ($S = 3/2$) and eight Mn₃₊ ($S = 2$) ions coupled by oxygen atoms. Beginning in 1988,¹⁹ the [Mn₁₂O₁₂(O₂CPh)₁₆(H₂O)₄] complex was studied and its ground state eventually determined^{20,21} to have $S = 10$. Note that this last system has 176 atoms

and 1210 electrons.

A major class of experimental effort has focused on design and synthesis of multi-nuclear clusters containing⁴ Mn^{3+} , because the axially Jahn-Teller distorted Mn^{3+} ions usually possess large magnetic anisotropy due to spin-orbital coupling. A large number of Mn(III)-based SMMs has been reported, including those with Mn_6 ²², Mn_{19} ²³⁻²⁵, Mn_{25} ^{26,27}, Mn_{31} ²⁸ and Mn_{84} ²⁹. In addition, inorganic chemists have also synthesized many transition metal (TM) SMMs based upon anisotropic V^{3+} , $\text{Fe}^{2+/3+}$, Ni^{2+} , and Co^{2+} ions; see Refs. 3, 30–35. The octa-nuclear cluster $[\text{Fe}_8\text{O}_2(\text{OH})_{12}](\text{tacn})_6^{8+}$ (Fe^8) reported by Sangregorio et al.³¹ is an example. It has 174 atoms and 756 electrons with an $S = 10$ ground state that arises from competing anti-ferromagnetic interactions between eight Fe^{3+} ($S = 5/2$) ions³⁶. Magnetic measurements revealed that it has an anisotropy barrier of 17 cm^{-1} , much smaller than that of Mn_{12} complexes. Another significant amount of synthesis effort has been focused on enhancing the magnetic anisotropy of the molecule³⁷⁻⁴⁰. That has stimulated the development of several different groups of SMMs such as cyano-bridged SMMs⁴¹⁻⁴³, Ln-based SMMs⁴⁴⁻⁴⁸, 3d-4f electron elements based SMMs^{46,49}, actinide-based SMMs⁴⁷, radical-bridged SMMs⁵⁰ and organo-metallic SMMs⁵¹.

The essential context for insightful computational studies illustrated by this brief overview is that SMMs are large, structurally and electronically complex molecules with complicated spin manifolds. Materials comprised of them are more complicated and demanding. Most of the chemical details of SMMs are largely irrelevant at this stage. However, the presence of heavy nuclei and the importance of anisotropy both implicate the significance of relativistic effects, including spin-orbit coupling. Predictive, materials-specific simulations of systems composed from SMMs thus are extremely challenging.

B. Predictive computational approaches

For the even-handed treatment of electronic structure of large condensed phase systems as well as their individual molecular constituents, at present the dominant first-principles approach is via density functional theory (DFT)⁵² in its Kohn-Sham (KS) variational form⁵²⁻⁵⁵. Typically the DFT calculation of the structural, energetic, and thermal-chemistry properties of a magnetic molecule (or crystal thereof) are followed by spin modelling in the form of the Heisenberg Hamiltonian or a related model, with the exchange coupling J being the

well-known key ingredient. Two major decisions go into the DFT calculations, the choice of exchange-correlation (E_{xc}) approximation and the choice of method for solving the resulting KS equations. We address only the second issue here. The first is the subject of intense investigation and development.

For determining the vibrational spectra and the temperature dependence of crystalline phases, the forefront practice today is to use *ab initio* molecular dynamics in the Born-Oppenheimer approximation (BOMD)^{56,57}. In BOMD, the ions move classically with electronic forces from DFT. The fastest general purpose implementation is to solve the KS equations in a plane-wave basis set, thereby avoiding artificial “Pulay” forces from an ion-centered basis functions. Even for static lattice calculations, the plane-wave basis offers the advantage that basis enrichment is systematic and simple, just increase the size of the largest wave-vector utilized. Furthermore, the plane-wave basis is unbiased with respect to ionic charge.

Since the early days of solid-state physics it has been known that the plane-wave basis becomes prohibitively large if the oscillations of one-fermion states near the nucleus caused by the bare Coulomb potential are included straightforwardly⁵⁸. The most widely used way to evade this problem is to replace the bare Coulomb potential with a pseudo-potential of some sort⁵⁹ or, more recently, projector augmented waves PAWs⁶⁰. For brevity in what follows, we refer to all such calculations as “plane-wave pseudo-potential”. Well-known, widely used examples of such codes include VASP⁶¹, QuantumEspresso⁶², and ABINIT^{63–65}.

Details of the specialized techniques involved with pseudo-potentials or PAWs are irrelevant here. What is relevant is that such calculations are not truly all-electron. Pseudo-potentials eliminate core states, while PAWs reconstruct them. In consequence it has become normative to test and cross-check plane-wave pseudo-potential calculations against truly all-electron calculations; for only three examples of many, see Refs. 66–68. Such cross-validation is particularly important in the context of molecular magnetic quantum materials because of core contributions to spin manifolds and relativistic contributions arising in non-trivial part from the core, e.g., spin-orbit interaction effects.

The all-electron methodology of choice is the full-potential, linearized augmented plane-wave (FLAPW) method or its close kin, APW+*lo*, augmented plane-wave plus local orbitals⁶⁹. The “full-potential” adjective refers to the use of the whole Kohn-Sham (KS) crystalline potential, not just the so-called muffin-tin (MT) part of it, historically an im-

portant distinction. Fig. 1 illustrates the MT decomposition as a 2D projection of a generic unit cell. The MT potential is spherically averaged in non-overlapping spheres centered upon each nucleus and averaged to a constant in the non-spherical remainder region (“interstitial”). In a modern context, it is used only to generate the radial part of the LAPW or APW+*lo* basis.

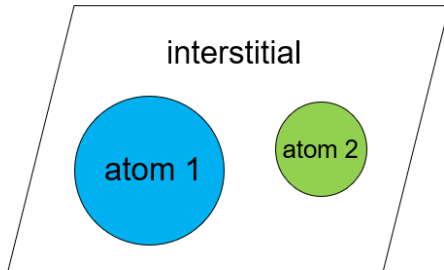


FIG. 1. Muffin-tin partitioning of a unit cell.

Both FLAPW and APW+*lo* are rooted in Slater’s original APW scheme^{70–75}. The physical motivation is that near a nucleus the MT potential resembles an atomic central-field potential very closely, whereas in the interstitial regime, the MT potential is constant. Within the MT spheres therefore, all three schemes (original APW, FLAPW, APW+*lo*) build basis functions that are atomic-like solutions of spherical potentials centered on each nucleus that are matched with plane waves in the interstitial region.

There is a substantial original literature about the FLAPW method,^{76–90} the addition of a particular kind of local orbital (“LO”, not “*lo*”) to it⁹¹ and the closely related APW+*lo* scheme⁹². Also there are at least two books^{69,93}, and various review chapters (e.g. Refs. 94 and 95). Therefore we do not review the entirety of the formulation here but display only those equations directly relevant to our discussion of codes and algorithmic libraries.

The original APW basis function for Bloch wave-vector \mathbf{k} and plane-wave vector \mathbf{G} is

$$\varphi_{\mathbf{k}}^{\mathbf{G}}(\mathbf{r}) := \begin{cases} \sum_{\ell, m} \sum_{\nu} A_{\ell m \nu}^{\alpha, \mathbf{k}}(\mathbf{G}) u_{\ell \nu}^{\alpha}(r) Y_{\ell m}(\hat{\mathbf{r}}) & , \mathbf{r} \in \alpha \\ (1/\sqrt{\Omega}) e^{i(\mathbf{G}+\mathbf{k}) \cdot \mathbf{r}} & , \mathbf{r} \notin \alpha \end{cases}$$

Here $u_{\ell \nu}^{\alpha}(r)$ is the solution of the (energy dependent) radial Schrodinger equation in the MT sphere labeled α ; $Y_{\ell m}(\hat{\mathbf{r}})$ are spherical harmonics; $A_{\ell m \nu}^{\alpha, \mathbf{k}}(\mathbf{G})$ are the matching coefficients for connection with the interstitial plane wave; ℓ and m are the azimuthal and magnetic

quantum numbers in a particular sphere; and ν is the order of energy derivative of the radial function (the APW basis set does not have continuous radial first derivatives at the sphere boundaries.) The dependence of the radial functions upon the energy for which they are solved is the difficulty with the APW basis set. Continuity at sphere boundaries requires those solution energies to correspond to KS eigenvalues. That correspondence makes the KS secular equation highly non-linear in the one-electron energies. The consequence is a significant computational burden, as well as difficult-to-manage singularities whenever a radial basis function has a node on a sphere boundary.

The LAPW basis addresses those difficulties by using both the radial functions $u(r; \epsilon_\ell)$ at reference energies ϵ_ℓ and their energy derivatives

$$\dot{u}_{\ell\nu} := \left. \frac{\partial u_{\ell\nu}(r; \epsilon)}{\partial \epsilon} \right|_{\epsilon_\ell} \quad (1)$$

in the basis set. (The “dotted” notation for the energy derivative is conventional in FLAPW literature.) Thus the basis functions become

$$\begin{aligned} \varphi_{\mathbf{k}}^{\mathbf{G}}(r) &:= \sum_{\ell, m} \sum_{\nu} [A_{\ell m \nu}^{\alpha, \mathbf{k}}(\mathbf{G}) u_{\ell\nu}^{\alpha}(r; \epsilon_\ell) + B_{\ell m \nu}^{\alpha, \mathbf{k}}(\mathbf{G}) \dot{u}_{\ell\nu}^{\alpha}(r, \epsilon_\ell)] Y_{\ell m}(\hat{\mathbf{r}}) \quad \mathbf{r} \in \alpha \\ &:= \frac{1}{\sqrt{\Omega}} \exp^{i(\mathbf{G}+\mathbf{k})\cdot\mathbf{r}} \quad \mathbf{r} \notin \alpha . \end{aligned} \quad (2)$$

The coefficients are determined by the requirement that each basis function be continuous with continuous first radial derivative at each sphere boundary. In the LAPW basis, the KS secular equation has the ordinary linear variational form, with the only issues of computational art being the choice of the reference energies ϵ_ℓ and muffin-tin radii. More recent literature^{96,97} sometimes does not separate the A and B matching coefficients; rather they are all under one name A , labeled with an index ν , the order of LAPW, to denote $u_\ell(r)$ and $\dot{u}_\ell(r)$ radial functions. Here we still follow the original LAPW notation for the coefficients A and B .

As the LAPW linearization is not unique, various other forms were tried⁹¹ including a local orbital scheme. Denoted “FLAPW + LO” (notice the upper case “LO”; it is important), one or more \mathbf{k} -independent local basis functions were added within a given sphere. Each such LO was a linear combination of two radial functions at different reference energies and a single energy derivative function. The coefficients of the three were determined by requiring that the resulting basis function vanish on the sphere surface, with vanishing derivative, plus normalization.

Later it was realized⁹² that a more efficient linearization is to use the original APW basis functions inside the sphere but at fixed reference energy and complement them with a set of linearized (in energy) radial functions that vanish on the sphere boundaries. Thus the “APW+*lo*” basis consists of Eq. (1) enhanced with different local orbitals (“lo”),

$$\varphi_{lo}(\mathbf{r}) := \sum_{\ell,m} \sum_{\nu} [A_{\ell m \nu}^{\alpha} u_{\ell \nu}^{\alpha}(r; \epsilon_{\ell}) + B_{\ell m \nu}^{\alpha} \dot{u}_{\ell \nu}^{\alpha}(r, \epsilon_{\ell})] Y_{\ell m}(\hat{\mathbf{r}}), \quad \mathbf{r} \in \alpha. \quad (3)$$

These localized basis functions do not have continuous derivatives at the sphere boundary, so surface terms arise in the kinetic energy and in any gradient-dependent exchange correlation functional.

The work presented here focuses upon LAPW (and LAPW+LO) and APW+*lo* implementations. The two basis sets can be used together with suitable reference energy choices and consideration of the atomic structure differences among spheres. Note also that both basis sets are adaptive, the radial functions evolve as the KS potential evolves from SCF iteration to iteration. Basis sets of the APW, FLAPW, APW+*lo* type cause the electron number density $n(\mathbf{r})$ and the KS effective potential $v_{KS}(\mathbf{r})$ to be adapted to the MT subdivision of the unit cell. In the interstitial region they are expanded in plane waves and inside MT spheres in real spherical harmonics $R_{\ell m}(\mathbf{r})$:

$$n(\mathbf{r}) = \begin{cases} \sum_{\ell m} n_{\ell m}^{\alpha}(r) R_{\ell m}(\hat{\mathbf{r}}), & \mathbf{r} \in \alpha \\ \sum_{\mathbf{G}} \tilde{n}(\mathbf{G}) e^{i\mathbf{G}\cdot\mathbf{r}}, & \mathbf{r} \notin \alpha \end{cases} \quad (4)$$

and

$$v_{KS}(\mathbf{r}) = \begin{cases} \sum_{\ell m} v_{\ell m}^{\alpha}(r) R_{\ell m}(\hat{\mathbf{r}}), & \mathbf{r} \in \alpha \\ \sum_{\mathbf{G}} \tilde{v}(\mathbf{G}) e^{i\mathbf{G}\cdot\mathbf{r}}, & \mathbf{r} \notin \alpha. \end{cases} \quad (5)$$

Here $n_{\ell m}^{\alpha}(r)$, $\tilde{n}(\mathbf{G})$, $v_{\ell m}^{\alpha}(r)$, and $\tilde{v}(\mathbf{G})$ are expansion coefficients determined through the self-consistent solution of the KS equation.

When the FLAPW methodology first came into use, there were several implementations in unpublished codes. Apparently the first publicly available code was WIEN⁹⁸, which over three decades has evolved into WIEN2K^{94,99}. Subsequently several other codes became widely available, notably ELK¹⁰⁰, FLEUR¹⁰¹, and *exciting*⁹⁶. The naming can be a bit confusing as both ELK and current *exciting* originated from the original instantiation, also called Exciting. Here we have in mind only the current *exciting*, not the original.

The present work focuses on a fork called *Exciting-Plus*, hereafter “EP” for brevity¹⁰². EP was developed from an early version of the ELK/*exciting* code, that was branched at the time when independent development of *exciting* and ELK had just begun. EP was developed with emphasis on post-ground-state calculations such as for the density response function¹⁰³ and RPA¹⁰² and GW¹⁰⁴ calculations. Ground state KS calculations are done with k -point task distribution and LAPACK¹⁰⁵ support. EP also implemented a convenient *mpi-grid* to control task parallelization in several independent variable dimensions, e.g. k -points, i - j index pairs of Kohn-Sham states, and q points in the calculation of the Kohn-Sham density response function.

While EP was constructed conscientiously in terms of coding practices, its design did not focus on large-system performance. The present work addresses that issue. Our goal is to retain the features and capabilities of EP while making it fast and efficient enough to make all-electron, full-potential DFT calculations routinely feasible for large, complicated systems such as magnetic molecules and their aggregates. The strategy is to use an optimized library for calculations common to all FLAPW-type basis schemes. In the following sections, we describe how we enhance the capabilities of EP by interfacing it to a powerful DFT-solver library called SIRIUS⁹⁷. After describing construction of the interface, we benchmark it using small bulk systems for verification, then demonstrate its utility by calculations on a selection of larger magnetic molecules that the original EP code cannot handle.

II. THE SIRIUS LIBRARY

Irrespective of the particular code, FLAPW/LAPW+*lo* calculations obviously have the same underlying formalism. Because the basic conceptualization starts with plane waves, those codes also share significant formal and procedural elements with plane-wave pseudo-potential (PW-PP) codes. Specifically the following tasks are shared: unit cell setup, atomic configurations, definition and generation of reciprocal lattice vectors \mathbf{G} and combinations with Bloch vectors $\mathbf{G} + \mathbf{k}$, definition of basis functions on regular grids as Fourier expansion coefficients; construction of the plane wave contributions to the KS Hamiltonian matrix, generation of the charge density, effective potential, and magnetization on a regular grid; symmetrization operations on the charge density, potential and occupation matrix; iteration-to-iteration mixing schemes for density and potential; diagonalization of the secular equation.

Compared to PW-PP codes, FLAPW/APW+*lo* additionally have everything expanded in radial functions and spherical harmonics inside the MT spheres, and enforcement of matching conditions on sphere surfaces.

From a development perspective, these commonalities offer an opportunity. Rather than have the developers of each individual code devise — and in many cases essentially reinvent — various schemes for computational speed and scalability, we can proceed via *separation of concerns*, identify the general calculation elements within the plane wave Kohn-Sham DFT formalism and create a library with explicit support for FLAPW/APW+*lo* and PW-PP calculations. By abstracting and encapsulating the common objects such as the examples just given, the focus then can be on optimizing computational performance. The SIRIUS library was created as such an optimized collection. It was designed from the outset with both task parallelization and data parallelization. It has been optimized for multiple MPI levels as well as OpenMP parallelization and also optimized for GPU utilization.

Although SIRIUS, as written, has basic FLAPW/LAPW+*lo* stand-alone capability, its primary usage is intended to be as a *DFT library* rather than another independent FLAPW code package. SIRIUS can be interfaced directly with both existing FLAPW/APW+*lo* codes and with PW-PP codes. Figure 2 demonstrates the difference between the traditional way of developing DFT applications based on mathematical libraries and the way the SIRIUS library is intended to be used to accelerate and enhance existing FLAPW/APW+*lo* and PW-PP codes. Note again the separation of concerns: only the essential elements of the ground-state KS problem expressed in a plane-wave type basis are addressed by SIRIUS.

The SIRIUS library is written in C++ in combination with the CUDA¹⁰⁶ backend to provide the following features: (1) low-level support such as pointer arithmetic and type casting as well as high-level abstractions such as classes and template meta-programming; (2) easy interoperability between C++ and widely used Fortran90; (3) full support from the standard template library (STL)¹⁰⁷; (4) easy integration with the CUDA nvcc compiler¹⁰⁸. The SIRIUS code provides dedicated API functions to interface to QuantumEspresso and *exciting*.

Importantly, the SIRIUS library is designed and implemented with both task distribution and data (large array) distribution in mind. Virtually all KS electronic structure calculations rely at minimum on two basic functionalities: distributed complex matrix-matrix multiplication (`pzgemm` in LAPACK) and a distributed generalized eigenvalue solver (`pzhgvx` also

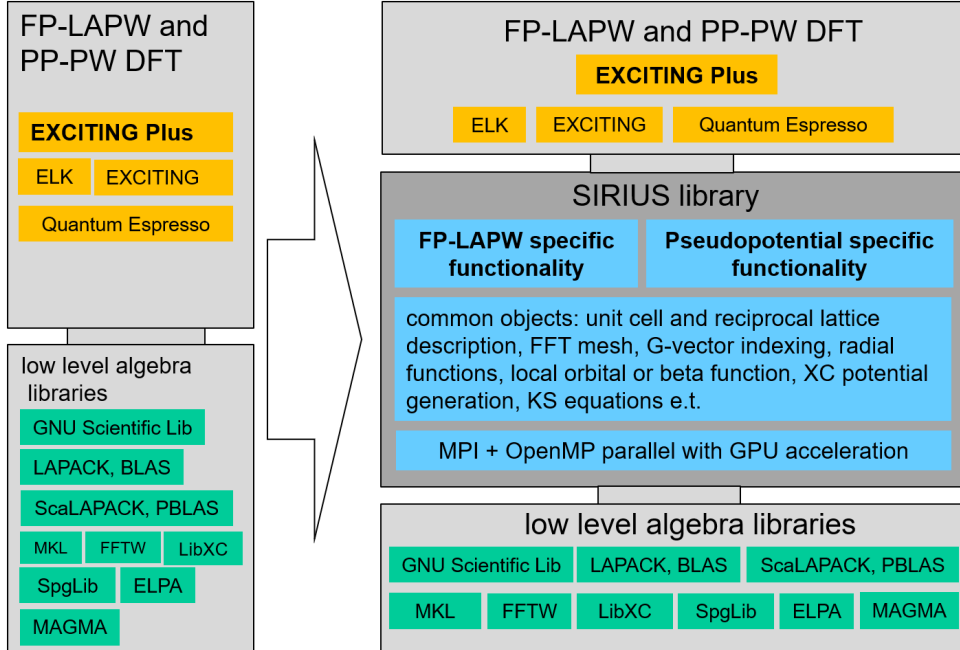


FIG. 2.

in LAPACK). SIRIUS handles these two major tasks with data distribution and multiple levels of task distribution.

The eigenvalue solver deserves scrutiny. Development of *exciting* revealed that considerable changes in code were required to scale the calculation to a larger number of distributed tasks, e.g. by making the code switchable from LAPACK to ScaLAPACK. This can be seen by comparing the task distribution and data distribution of the base ground state subroutine in recent versions of *exciting* (version Nitrogen for example) and ELK (version 5.2.14 or earlier version for example). Evidently the ELK developer team had emphasized physics features and functionalities rather than adding support for ScaLAPACK. The situation with EP is similar to that of ELK. EP has only LAPACK support and does not have data distribution of large arrays. Table I summarizes the diagonalization methods available in these codes.

Eigenvalue solver performance is well known to be quite dependent upon limitations of the underlying algorithms. Widely used linear algebra libraries such as LAPACK and ScaLAPACK implement robust full diagonalization algorithms that can handle system

TABLE I. Eigensolver options

	full diagonalization		iterative diagonalization
	LAPACK	ScaLAPACK	Davidson algorithm
Exciting-Plus	Yes	No	No
ELK	Yes	No	Yes
<i>exciting</i>	Yes	Yes	Yes
SIRIUS	Yes	Yes	Yes

size up to about 10^6 . But, unfortunately, the very large plane wave cutoff needed for FLAPW/APW+*lo* calculations on systems as large as 100+ atoms, the eigensystem often is several times larger than that. A Davidson-type¹⁰⁹ iterative diagonalization algorithm is often suitable for such large systems because it suffices to solve for the lowest 10–20 percent of all eigenvalues and the associated eigenvectors to obtain the valence band structure around the Fermi energy. But Davidson-type diagonalization algorithms are not offered in standard linear algebra libraries. That omission is at least in part because such algorithms involve repeated application of the Hamiltonian to a sub-space of the system. Thus the algorithm depends on construction details of the Hamiltonian matrix, i.e. it depends on the specific DFT formalism. The SIRIUS library takes this into consideration and offers an efficient implementation of Davidson-type diagonalization¹¹⁰ for FLAPW/APW+*lo* and PW-PP codes .

III. INTERFACING EXCITING-PLUS WITH SIRIUS

Despite its many attractive features, especially for post-ground state calculations that are increasingly important, EP has some significant limitations in regard to large systems. Particularly for the ground state calculation, EP is limited by: (1) provision of only the LAPACK eigensolver; and (2) *k*-point-only MPI parallelization (which makes the code completely serial for single *k*-point calculations, e.g. an isolated molecule). Interfacing to the SIRIUS library would remove these limitations with minimal code modification. Thus our approach is completely straight-forward. We outsource the ground-state self-consistent KS solution problem to SIRIUS. The result is that the ground-state calculation of SIRIUS-enhanced-EP has powerful eigensystem solver support and an additional level of task parallelizations:

(a) ScaLAPACK support; (b) Davidson iterative eigensolver; (c) band MPI parallelization within one k -point; and (d) thread-level OMP parallelization per k -point per band. The user interface however, remains as essentially unaltered EP.

Implementation of the interface benefits from the FORTRAN API functionalities provided by SIRIUS. The listings that follow display the FORTRAN API function calls for parsing the atomic configuration, the APW basis, and the lo basis from EP, and passing them to SIRIUS:

Listing 1. setting up atomic configuration

```
do ist = 1, spnst(is)
  call sirius_set_atom_type_configuration(sctx, string(trim(label)),&
    & spn(ist,is), spl(ist,is), spk(ist,is), spocc(ist,is),&
    & logical(spcore(ist,is),kind=c_bool))
enddo
```

This piece of code loops over the number of states of a single type of atom (`spnst`: species' number of states). For each state, the API call parses the following information to SIRIUS: quantum numbers n , l and k for each state (`spn`, `spl` and `spk`), occupation of that state (`spocc`), and whether that state is treated as core state (`spcore`).

Listing 2. Fortran API for basis description

```
! parsing APW descriptions from host code to SIRIUS
do l = 0, lmaxapw
  do io = 1, apword(l, is)
    autoenu = .false.
    if (use_sirius_autoenu.and.apwve(io,l,is)) autoenu = .true.
    call sirius_add_atom_type_aw_descriptor(sctx, string(trim(label)),&
      &apwpqn(l,is), l, apwe0(io, l, is), apwdm(io, l, is),&
      &logical(autoenu,kind=c_bool))
  enddo
enddo
! parsing LO/lo description from host code to SIRIUS
```

```

do ilo = 1, nlorb(is)
  do io = 1, lorbord(ilo, is)
    autoenu = .false.
    if (use_sirius_autoenu.and.lorbve(io, ilo, is)) autoenu = .true.
    call sirius_add_atom_type_lo_descriptor(sctx, string(trim(label)),&
      &ilo, lopqn(ilo,is), lorbl(ilo, is),lorbe0(io, ilo, is),&
      &lorbdm(io, ilo, is), logical(autoenu,kind=c_bool))
  enddo
enddo

```

The chunk of code above contains two double loops. The first one loops over the APWs of one atom type and the ℓ -channels of each APW. For each ℓ -channel, the API call parses the following information to SIRIUS: the principle quantum numbers n (`apwpqn`), the value of l (`l`), the value of the initial linearization energy (`apwe0`), the order of energy derivative of that APW (`apwdm`), and whether the linearization energy is allowed to be adjusted automatically (`autoenu`). The second double loop is over the total number of local orbitals (`nlorb`) of one atom type and the *orders* (`lorbord`) of each local orbital (i.e. number of $u(r)$ or $\dot{u}(r)$ terms in that local orbital). The API call parses the following information to SIRIUS: quantum numbers n and l (`lopqn` and `lorbl`), initial linearization energy (`lorbe0`), order of energy derivative (`lorbdm`) and whether the linearization energy is allowed to be adjusted automatically (`autoenu`).

General input parameters such as the plane-wave cutoff, ℓ cutoff for the APWs and for density and potential expansion, \mathbf{k} -points, lattice vectors and atom positions, etc., all are set as usual in the EP input file. Then they are parsed to SIRIUS via its built-in *import* and *set parameter* functionalities. Other important parameters such as the fast Fourier transform grid, radial function grid inside each MT sphere and number of first variational states⁶⁹ often are not set in EP input files but defaulted. Instead, those also *must* be parsed to SIRIUS in the initialization step to ensure that the Hamiltonian matrix and eigenvectors are exactly same size in both EP and SIRIUS. There is other information, such as specification of core states, linearization energy values, and MT radii defined in the so-called species files of EP, that also is parsed during the calculation to SIRIUS to overwrite the corresponding default

values in EP.

Listing 3. Fortran API for setting inputs for SIRIUS

```
call sirius_set_parameters( sctx,&
                           &use_symmetry=bool(.true.),&
                           &valence_rel=string('zora'),&
                           &core_rel=string('none'),&
                           &auto_rmt=0,&
                           &fft_grid_size=ngrid(1),&
                           &num_mag_dims=ndmag,&
                           &num_fv_states=nstfv,&
                           &pw_cutoff=gmaxvr,&
                           &gk_cutoff=gkmax,&
                           &lmax_apw=lmaxapw,&
                           &lmax_rho=lmaxvr,&
                           &lmax_pot=lmaxvr      )
```

This chunk of code is an example of basic inputs that are added in EP. Most of the meanings are explicit in the name. `zora` means zero order relativistic approximation. `ngrid` is the FFT grid set up in EP and parsed to SIRIUS. Plane wave cutoff and $|G + k|$ cutoff are `gmaxvr` and `gkmax` in EP. The `lmaxapw` and `lmaxvr` are angular momentum cutoff for APW and for charge density (and potential) inside MT.

Listing 4. eigen solver selection and Davidson solver parameter setup

```
if (sirius_davidson_eigen_solver) then
  call sirius_import_parameters(sctx, string('{"iterative_solver" : {"type"
      : "davidson" }}'))
  call sirius_import_parameters(sctx, string('{"iterative_solver" :
      {"energy_tolerance" : 1e-13}}'))
  call sirius_import_parameters(sctx, string('{"iterative_solver" :
      {"residual_tolerance" : 1e-6}}'))
  call sirius_import_parameters(sctx, string('{"iterative_solver" : {"num_steps"
```

```

        : 32}}'))
call sirius_import_parameters(sctx, string('{"iterative_solver" :
    {"subspace_size" : 8 }}'))
call sirius_import_parameters(sctx, string('{"iterative_solver" :
    {"converge_by_energy" : 1 }}'))
call sirius_import_parameters(sctx, string('{"iterative_solver" :
    {"num_singular" : 20 }}'))
else
    ! otherwise use full eigen solver from LAPACK
    call sirius_set_parameters(sctx, iter_solver_type=string('exact'))
endif

```

The code above is added to supply additional parameters for Davidson method if it is used. After ensuring that the setup of input quantities is identical between the host code, i.e. EP, and SIRIUS, the ground state calculation is completely done by SIRIUS. The results, eigenvalues and eigenvectors, are parsed back to the host code for further calculation. The chunk of code below displays the typical API calls to retrieve the resulting eigenvalues and eigenvectors.

Listing 5. Fortran API for retrieving eigen values and eigen vectors from SIRIUS

```

! get local fraction of eigen-vectors
do ikloc=1,nkptloc
    ik=mpi_grid_map(nkpt,dim_k,loc=ikloc)
    call sirius_get_fv_eigen_vectors(ks_handler, ik, evecfvloc(1, 1, 1, ikloc),
        nmatmax, nstfv)
    call sirius_get_sv_eigen_vectors(ks_handler, ik, evecsvloc(1, 1, ikloc), nstsv)
enddo !ikloc
! get all eigen-values and band occupancies
do ik = 1, nkpt
    if (ndmag.eq.0.or.ndmag.eq.3) then
        call sirius_get_band_energies(ks_handler, ik, 0, evalsv(1, ik))
    end if
enddo

```

```

    call sirius_get_band_occupancies(ks_handler, ik, 0, occsv(1, ik))
else
    call sirius_get_band_energies(ks_handler, ik, 0, evalsv(1, ik))
    call sirius_get_band_energies(ks_handler, ik, 1, evalsv(nstfv+1, ik))
    call sirius_get_band_occupancies(ks_handler, ik, 0, occsv(1, ik))
    call sirius_get_band_occupancies(ks_handler, ik, 1, occsv(nstfv+1, ik))
endif
enddo

```

One needs to be very careful in dealing with the MPI task schedules when interfacing to SIRIUS library because most likely the host code has a MPI implementation that is different from SIRIUS. For our case, it is relatively straightforward because EP has only k -point parallelization in the ground state calculation. In the initialization step, we set the SIRIUS MPI communicator to be derived from global MPI communicator (MPI_COMM_WORLD) of the host code so that all MPI ranks will be used by SIRIUS. Then user needs to specify how SIRIUS will carry out k -point distribution, how to plan further band parallelization within a k -point and thread level parallelization. The schedule of k -point parallelization and band parallelization are required additional inputs. Thread level parallelization is also additional inputs, which are specified in run job script. After SIRIUS finishes the ground state calculation, before calling the API to parse eigenvalues and eigenvectors back to EP, SIRIUS will do *mpi_reduce* in the MPI band dimension and prepare full eigenvalues and eigenvectors by k -points and by (the same) global k -point index. The last piece of the interface is the additional inputs for the SIRIUS Davidson diagonalization algorithm. These are adjustable numerical parameters and directly parsed over by EP.

The MPI parallelization in the band degree of freedom is one major gain of interfacing to SIRIUS. As mentioned before, EP would run completely in non-parallel mode if the job is a single k -point calculation, which is often used when people study isolated systems. The SIRIUS-enhanced-EP turns out to have the same scaling as SIRIUS alone, as expected, in the case of single k -point calculations. Figure 3 displays the benchmark of band-parallelization using the DTN molecule, which has 70 atoms. The molecule is placed in a 10 \AA cube unit cell, with plane wave cutoff $20 a_0^{-1}$ and angular momentum cutoff 7. All jobs are set to 16

multi-threads in one task to meet the hardware configuration. The recorded time is for the 1st 100 SCF iterations using the Davidson diagonalization eigensolver.

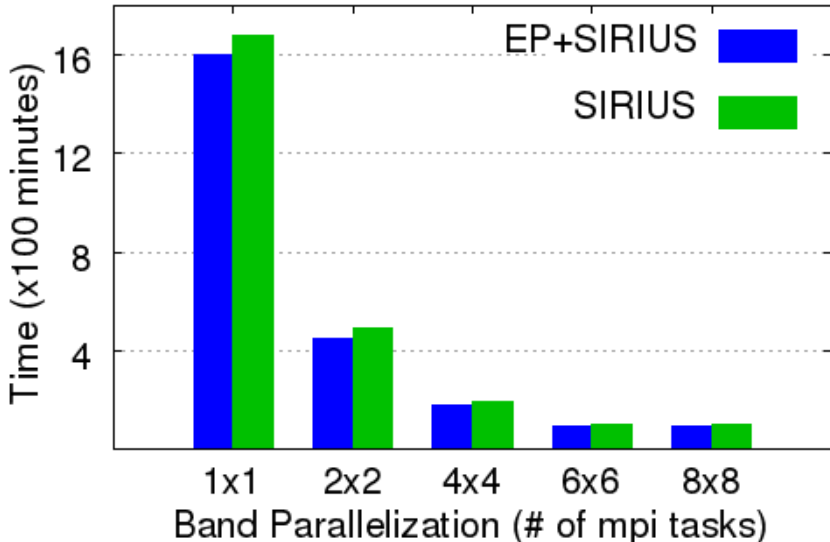


FIG. 3. Benchmark of band parallelization in single k -point jobs. $n \times n$ ranks are used for one k -point.

IV. EP+SIRIUS: VERIFICATION TESTS ON SMALL SOLID STATE SYSTEMS

The EP code interfaced with SIRIUS was first benchmarked against SIRIUS standalone, for small bulk systems. Ground state calculations for the simple bulk materials Al, Ni, Fe, NiO, C, Si, Ge, and GaAs are carried out to get the total energy (and magnetization if the system is magnetic) using the interfaced code. For each system the exactly same input parameters are used for the SIRIUS and EP+SIRIUS runs. We have adopted the experimental lattice parameters for all systems. The APW+ lo and LAPW bases were used, and LDA and GGA-PBE have been utilized for the exchange-correlation functionals. When

expanding the interstitial potential and charge density, the maximum length of the reciprocal lattice vector $|G|$ is used as plane wave cut-off for the APW, which is set to $12 a_0^{-1}$ (inverse Bohr radius) for all systems. The angular momentum has been truncated at $l_{\max} = 8$ for APW. The same angular momentum cut is used for the charge density, potential, and wave function inside the muffin-tin. The linearization energy, which is associated with each radial function of APW, is chosen at the center of the corresponding band with l -like character for all systems. The first BZ has been sampled by a dense $16 \times 16 \times 16$ k -mesh for all systems. All parameters have been carefully tested to achieve total energy convergence. For the EP+SIRIUS calculations, the diagonalization method is always switched to the Davidson iterative eigensolver.

Table II summarizes the APW+ lo basis configuration, settings other than the cuts mentioned above, and the converged total energy and magnetization of these small systems. Table III summarizes the same calculation setup with the LAPW basis. The good agreements in total energy and magnetization in these tests validate that the identical basis setup is realized and the constructed interface carries the original SIRIUS calculation over into the host code.

TABLE II. EP+SIRIUS vs. SIRIUS, using APW+*lo*

	Al (non-mag.)	NiO (non-mag.)	Ni (FM)	Fe (FM)
crystal structure	fcc	rock-salt	fcc	bcc
latt. const. (Å)	4.05	4.17	3.52	2.87
R_{mt} (a_0)	1.8	1.8, 1.6	2.0	2.0
valence relativity	z.o.r.a.	z.o.r.a.	z.o.r.a.	z.o.r.a.
<i>lo</i> config. ★	Al: <i>s, p</i>	Ni: <i>s, p, d</i> O: <i>s, p, d</i>	Ni: <i>s, p, d</i>	Fe: <i>s, p, d</i>
LO for semi-core ★★	$\epsilon'_{2p} = -2.55$	$\epsilon'_{Ni,3d} = -0.33$ $\epsilon'_{O,2s} = -0.87$	$\epsilon'_{Ni,3d} = -0.33$ $\epsilon'_{Ni,3p} = -2.59$	$\epsilon'_{Fe,3d} = -0.28$ $\epsilon'_{Fe,3p} = -2.18$ $\epsilon'_{Fe,3s} = -3.43$
treated as core state	1s, 2s	Ni: 1s,2s,2p,3s O: 1s	1s,2s,2p,3s	1s,2s,2p
LDA: (unit: Ha, μ_B)				
E_{tot} , SIRIUS	-241.40085447	-1593.13659104	-1518.09194282	-1270.11766996
E_{tot} , EP+SIRIUS	-241.40085447	-1593.13659102	-1518.09194282	-1270.11766997
μ_{tot} , SIRIUS			0.564822	2.308247
μ_{tot} , EP+SIRIUS			0.564825	2.308245
GGA-PBE: (unit: Ha, μ_B)				
E_{tot} , SIRIUS	-241.54245824	-1593.27058366	-1518.15356943	-1270.18442575
E_{tot} , EP+SIRIUS	-241.54245824	-1593.27058365	-1518.15356942	-1270.18442575
μ_{tot} , SIRIUS			0.563466	2.327534
μ_{tot} , EP+SIRIUS			0.563467	2.327530

TABLE III. EP+SIRIUS vs. SIRIUS, using LAPW

	Al (non-mag.)	NiO (non-mag.)	Ni (FM)	Fe (FM)
R_{mt} (a_0)	1.8	1.8, 1.6	2.0	2.0
	LAPW has same linearization energy as APW. No more lo configurations. LO configuration is same as Table-2. other parameters are also same as in Table-2			
LDA: (unit: Ha, μ_B)				
E_{tot} , SIRIUS	-241.40085321	-1593.13659761	-1518.09194596	-1270.11766882
E_{tot} , EP+SIRIUS	-241.40085422	-1593.13659902	-1518.09194752	-1270.11766822
μ_{tot} , SIRIUS			0.564830	2.308243
μ_{tot} , EP+SIRIUS			0.564827	2.308240
GGA-PBE: (unit: Ha, μ_B)				
E_{tot} , SIRIUS	-241.54245124	-1593.27058546	-1518.15356717	-1270.18442211
E_{tot} , EP+SIRIUS	-241.54245372	-1593.27058701	-1518.15356932	-1270.18442394
μ_{tot} , SIRIUS			0.563460	2.327533
μ_{tot} , EP+SIRIUS			0.563466	2.327528

V. EP+SIRIUS: MN-TAA MOLECULE

The so-called Mn(taa) molecule ($[Mn^{3+}(pyrol)_3(tren)]$) is a meridional pseudo-octahedral chelate complex of a single Mn as the magnetic center and the hexadentate tris[(E)-1-(2-azoly)-2-azabut-1-en-4-yl]amine ligand. It is a spin-crossover system of long-standing interest. Originally studied by Sim and Sinn¹¹¹, it was the first known example of a manganese(III) d^4 spin-crossover system. Experimentally it is found that the Mn^{3+} cation goes from a low-spin state to a high-spin state (HS) at a transition temperature of about 45K. The Mn(taa) structure is sufficiently large that it has non-negligible intra-molecular dispersion interactions with a critical HS-LS difference. The HS state involves anti-bonding molecular orbital occupation, hence the octahedral HS complex tends to have weaker and therefore longer metal-ligand bonds than the LS bonds. Therefore, the dispersion contribution to the metal-ligand bonding is lower for the HS case than for the more compact LS state. Mn(taa) poses challenges to the computational determination of the ground state because the purely molecular (non-thermal) $\Delta E_{HL} := E_{HS} - E_{LS}$ is small compared to the total energies. Estimates are about 50 ± 30 meV but as high as a few hundred meV.

Mn(taa) poses challenges to the computational determination of the ground state because ΔE_{HL} is small compared to the cohesive energy. Several factors that can significantly affect a DFT calculation of ΔE_{HL} of the molecule. For consistency with condensed phase calculations, it is appropriate to study the isolated molecule in a large, periodically bounded box. To ensure accuracy, the plane wave cutoff needs to be sufficiently large, and the amount of vacuum in the unit cell requires an larger-still cutoffs. We note that the usual GGA density functional approximations, such as PBE, suffer from a self-interaction error, hence they tend to favor the LS state to reduce that spurious self-repulsion with the result of overestimated ΔE_{HL} values. That is not of concern here since what we are testing is algorithmic efficiency.

For the test of EP + Sirius, we used the experimentally determined HS and LS Mn(taa) structures and did PBE calculations (no Hubbard U). The same structures were used also in a VASP calculation, also with PBE and without U . The total energy of LS state is determined to be about 412 meV below the HS state in both cases.

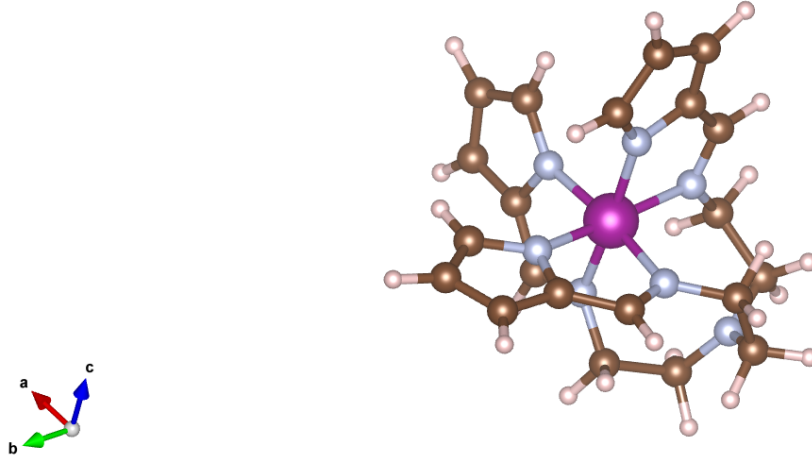


FIG. 4. Mn-taa molecule

TABLE IV. Complete input parameters for the Mn-taa LS state

structure	Mn-taa, LS state structure
unit cell	$20 \times 20 \times 20$ Angs box
number of atoms in unit cell	55
R_{mt} (a_0)	Mn: 2.2; O: 1.6; C: 1.4; H: 1.0;
G_{max} (a_0^{-1}) for APW	30
l_{max} for APW and ρ , (l_{max}^{APW} and l_{max}^ρ)	8
l_{max} for V_{eff} , (l_{max}^{pot})	8
k -points grid	$1 \times 1 \times 1$
(L)APW configuration for $l \leq l_{max}^{APW}$	$\epsilon_l = -0.15$ eV; $\partial_E = 0$;
lo configuration \star	Mn: s, p, d ; O/C: s, p ; H: s ;
LO for semi-core $\star\star$	$\epsilon'_{Mn,3d} = -0.32$; $\epsilon'_{Mn,3p} = -2.45$
treated as core state	Mn: 1s,2s,2p,3s; O/C: 1s
E_{tot} (Ha)	-35681.48593827
μ_{tot} (μ_B)	total: 2.00 Mn atom: 1.68

VI. EP+SIRIUS: DTN MOLECULE

The insulating organic compound $\text{NiCl}_2\text{-}[\text{SC}(\text{NH}_2)_2]_4$ (DTN molecule) is a molecule-based material in which magnetic and electric order can couple with each other. It has been experimentally studied for its quantum magnetism¹¹²⁻¹¹⁵. ($\text{NiCl}_2\text{-}[\text{SC}(\text{NH}_2)_2]_4$) has a tetragonal molecular crystal structure with two Ni atoms as magnetic centers in one unit cell. Each Ni has four S atoms and two Cl atoms as nearest neighbors, forming an octahedral structure (similar to the BO_6 octahedra in ABO_3 perovskites). The $\text{NiCl}_2\text{-}[\text{SC}(\text{NH}_2)_2]_4$ molecules pack in a body-centered tetragonal structure, with Ni-Cl-Cl-Ni bonding along the *c*-axis and hydrogen bonding between thiourea molecules in the *ab*-plane. The four thiourea molecules surrounding each Ni ion are electrically polar. The components of the thiourea electric polarization in the *ab*-plane cancel each other, while the *c*-axis components are in the same direction and create a net electric polarization along *c*-axis that could be responsible for magnetic field-modified ferroelectricity.

At temperatures below 1.2K and below a critical magnetic field, DTN is a quantum paramagnet. As the magnetic field, applied perpendicular to the *ab*-plane, reaches the first critical field, it experiences a quantum phase transition into an XY-antiferromagnetic (XY-AFM) state where all Ni spins lie within the *ab*-plane. When the field is increased further the spins begin to cant, with a corresponding increase in magnetization. When a second critical field is reached, the magnetization saturates and the material enters a spin-polarized state where all spins are pointing along the *c*-axis and parallel to the applied magnetic field. Recent DFT study¹¹⁶ has shown sufficiently large Coulomb interaction U of about 5-6 eV is needed to capture the essential physics. Using EP+SIRIUS, without U , we can converge to an AFM ground state of DTN, which is not the paramagnetic ground state observed in experiments. The calculation is only for benchmark purpose.

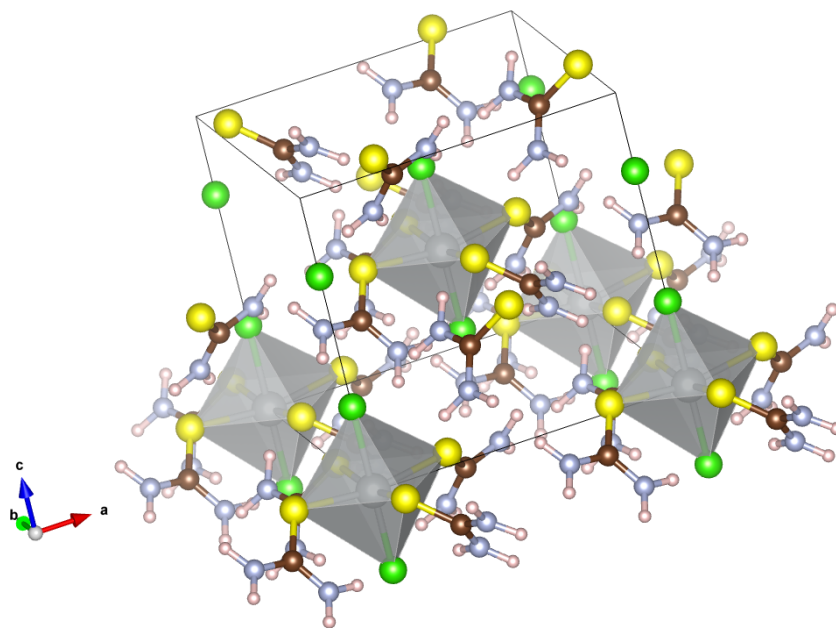


FIG. 5. DTN molecule crystal

TABLE V. Input parameters and outputs of DTN

	DTN
unit cell	$10 \times 10 \times 10$ Angs cubic
number of atoms in unit cell	70
R_{mt} (a_0)	Na: 2.2; Cl/S: 1.4; C: 1.2; H: 1.0;
G_{\max} (a_0^{-1}) for APW	25
l_{\max} for APW, (l_{\max}^{APW})	8
l_{\max} for ρ , (l_{\max}^{ρ})	8
l_{\max} for V_{eff} , (l_{\max}^{pot})	8
k -points grid	$1 \times 1 \times 1$
(L)APW configuration for $l \leq l_{\max}^{\text{APW}}$	$\epsilon_l = -0.15$ eV; $\partial_E = 0$;
lo configuration \star	Na: s, p, d Cl/S/C/N: s, p ; H: s
LO for semi-core $\star\star$	$\epsilon'_{Ni,3d} = -0.28$ $\epsilon'_{Ni,3p} = -2.18$
treated as core state	Ni: 1s,2s,2p,3s Cl/S/C/N: 1s
E_{tot} (Ha)	-168710.54331686
μ_{tot} (μ_B)	total: 0.0 Ni atom: +/- 1.42

VII. EP+SIRIUS: $[\text{Mn}_3]_2$ MOLECULE

A highly desirable property of SMMs for potential applications is the quantum mechanical coupling of two or more SMMs to one other or to a surface or other device component, all the while maintaining their isolated system magnetic properties. An SMM-SMM coupled structure has been identified for hydrogen-bonded supramolecular pairs of $S = 9/2$ SMMs $[\text{Mn}_4\text{O}_3\text{Cl}_4(\text{O}_2\text{CEt})_3(\text{py})_3]^{117-119}$. Since inter-SMM interactions based on hydrogen bonding

do not provide easy control of oligomerization nor guarantee retention of the oligomeric structure in solution, covalent organic linked SMM-SMM structures were developed. The first development in this direction was the $[\text{Mn}_3]_4$ tetramer of SMMs¹²⁰, which is covalently linked with dioximate linker groups.

A recent further development in this direction is the $[\text{Mn}_3]_2$ dimer molecule¹²¹. It is the largest system we have treated with all-electron DFT calculations. It is comprised of two Mn_3 units covalently joined via dpd2-dioximate linkers. The two triangular Mn_3 units are parallel, with each having the magnetic $S = 6$ ground state from intra- Mn_3 ferromagnetic couplings. The inter- Mn_3 interaction also has been determined to be ferromagnetic. There is no experimental evidence for noticeable interactions (dipolar or super-exchange) between the two dimers. That is consistent with the absence of significant inter-dimer contacts in the structure and the relatively large distance between Mn ions in adjacent dimers. The interaction quantum mechanically couples the two Mn_3 units. The structure is robust and resists any significant deformation or distortion that might affect the weak inter- Mn_3 coupling.

Once again, we treated the system as an isolated molecule in a box. The G_{max} cutoff and LO/*lo* configuration for Mn atoms were the same as for Mn_{taa} . We use the experimental structure and did DFT calculations with the PBE exchange correlation functional (again, no Hubbard U).

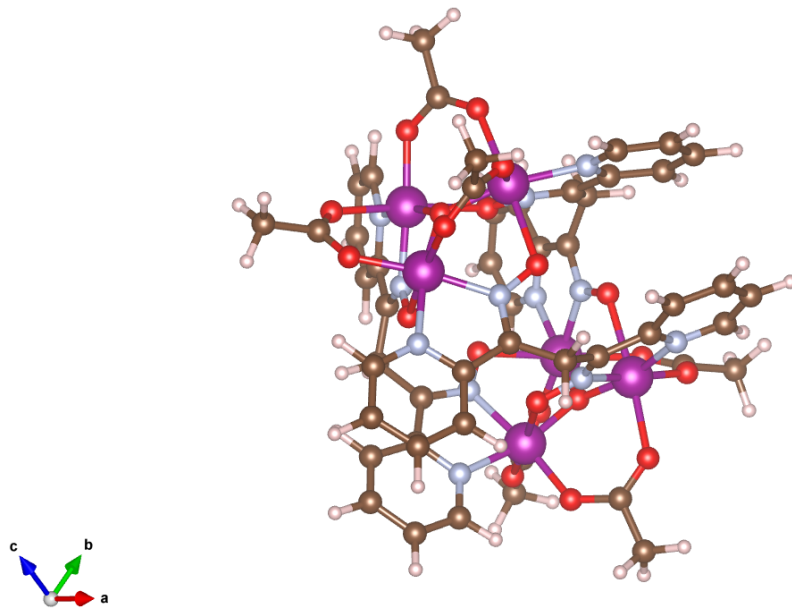


FIG. 6. Mn₃ dimer molecule

TABLE VI. Input parameters and outputs of Mn₃ dimer

	Mn ₃ dimer
unit cell	20 × 20 × 20 Angs cubic
number of atoms in unit cell	142
XC functional	GGA-PBE
R_{mt} (a_0)	Mn: 2.2; O: 1.4; C: 1.2; H: 1.0;
G_{\max} (a_0^{-1}) for APW	30
l_{\max} for APW, (l_{\max}^{APW})	8
l_{\max} for ρ , (l_{\max}^{ρ})	8
l_{\max} for V_{eff} , (l_{\max}^{pot})	8
k -points grid	1 × 1 × 1
(L)APW configuration for $l \leq l_{\max}^{\text{APW}}$	$\epsilon_l = -0.15$ eV; $\partial_E = 0$;
lo configuration ★	Mn: s, p, d Cl/S/C/N: s, p ; H: s
LO for semi-core ★★	$\epsilon'_{Mn,3d} = -0.32$ $\epsilon'_{Mn,3p} = -2.45$
treated as core state	Mn: 1s,2s,2p,3s O/C/N: 1s
E_{tot} (Ha)	-374249.74869342
μ_{tot} (μ_B)	total: 12.0 Mn atom: +1.79

VIII. SUMMARY AND CONCLUSION

To summarize, we have implemented a major enhancement of the Exciting-Plus FLAPW code by interfacing it with the SIRIUS library. The combination provides performance gains through diagonalization and parallelization improvements while retaining the user interface and post-processing functionalities of EP. The result is a major advance in capability for treating large, complex molecular aggregates.

In detail, the eigenvalue solver in Exciting-Plus is one major bottleneck in calculations of large systems, as the LAPACK full diagonalization algorithm cannot handle Hamiltonian matrices larger than $\sim 10^6$. By interfacing to the SIRIUS library, we provide the options to use of the various (LAPACK, ScaLAPACK, Davidson) diagonalization algorithms offered by SIRIUS. By setting up exactly the same basis functions provided by the Fortran API, for typical Kohn-Sham ground state calculations in condensed matter and molecular structures, one can easily perform Davidson-type diagonalization of the Hamiltonian in the self-consistent loop and benefit from multiple level parallelization within k -points and bands. The original Exciting-Plus input file can be used directly, adding only a few lines to switch on the usage of SIRIUS and to specify the additional parameters for the Davidson eigensolver. The eigenvalues and eigenvectors resulting from the SIRIUS calculation have the same structure as those of Exciting-Plus and they are transferred back to the host code. The entire interfaced code essentially embeds a SIRIUS SCF loop inside Exciting-Plus. The effort involved is relatively small, benefiting from the similarity of the data structures between Exciting-Plus and the FLAPW elements of SIRIUS.

For testing and validation, we showed results from small bulk systems calculated in both the APW+ lo basis and the LAPW basis. The resulting total energy and magnetization show no meaningful deviation from the SIRIUS standalone runs. Three very much larger molecular systems were calculated using the APW+ lo basis and the resulting magnetizations found to be in agreement with experimental measurements. In these test calculations, good scaling in band parallelization for a single k -point is observed, particularly for the larger molecules. The results also indicate that parallelization of the interfaced code works well on supercomputers, and the computational time is drastically reduced in comparison with the original Exciting-Plus. The main advantage of the interfaced code is the easiness of its construction and the support from advanced eigensolvers. We expect a similar interface

construction can be done with the ELK code or the EXCITING code without much extra effort.

Looking ahead, we have found that the non-distributed large arrays defined in the host code have become the new bottleneck. That is especially the case when dealing with molecular systems containing more than ≈ 100 atoms in a large unit cell. The primary cause of the bottleneck is the large plane wave G cutoff for large systems, and the fact that some fundamental multi-dimensional arrays are defined with one dimension containing all indices of the G vector or $G + k$ vector. Examples of such fundamental quantities include the augmentation wave part ($u \cdot Y_{lm}$ part) of the APW basis and the so-called structure factor, the form $\exp[i(G + k) \cdot r]$. These basic quantities are used in many places in the host code. It is not an easy job to change them to be distributed data in all occurrences. Although the limitation of the system size is still present, calculations based on the current interfaced code can handle larger systems than the original Exciting-Plus and offer a significantly improved foundation for examining the validity of the results from calculations based on various pseudo-potentials.

Acknowledgment This work is supported as part of the Center for Molecular Magnetic Quantum Materials, an Energy Frontier Research Center funded by the U.S. Department of Energy, Office of Science, Basic Energy Sciences under Award No. DE-SC0019330. Computations were performed at NERSC and the University of Florida Research Computer Center.

REFERENCES

- ¹M. R. Wasielewski, M. D. E. Forbes, N. L. Frank, K. Kowalski, G. D. Scholes, J. Yuen-Zhou, D. E. F. Marc A. Baldo, R. H. Goldsmith, T. G. III, M. L. Kirk, J. K. McCusker, J. P. Ogilvie, D. A. Shultz, S. Stoll, and K. B. Whaley, “Exploiting chemistry and molecular systems for quantum information science,” *Nature Reviews Chemistry* **4**, 490–504 (2020).
- ²A. Gaita-Ariño, F. Luis, s. Hill, and E. Coronado, “Molecular spins for quantum computation,” *Nature Chemistry* **11**, 301–309 (2019).
- ³S. L. Castro, Z. Sun, C. M. Grant, J. C. Bollinger, D. N. Hendrickson, and G. Christou, “Single-molecule magnets: Tetranuclear vanadium(iii) complexes with a butterfly structure and an $s = 3$ ground state,” *Journal of the American Chemical Society* **120**, 2365–2375 (1998), <https://doi.org/10.1021/ja9732439>.
- ⁴R. Bagai and G. Christou, “The drosophila of single-molecule magnetism: [mn12o12(o2cr)16(h2o)4],” *Chem. Soc. Rev.* **38**, 1011–1026 (2009).
- ⁵C. Marrows, L. Chapon, and S. Langridge, “Spintronics and functional materials,” *Materials Today* **12**, 70–77 (2009).
- ⁶J. R. Friedman and M. P. Sarachik, “Single molecule nanomagnets,” *Annual Review of Condensed Matter Physics* **1**, 109–128 (2010), <https://doi.org/10.1146/annurev-conmatphys-070909-104053>.
- ⁷P. L. Feng and D. N. Hendrickson, “Isostructural single-chain and single-molecule magnets,” *Inorganic Chemistry* **49**, 6393–6395 (2010), pMID: 20565068, <https://doi.org/10.1021/ic101016t>.
- ⁸J. L. Rong-Min Wei, Fan Cao, “Single-chain magnets based on octacyanotungstate with the highest energy barriers for cyanide compounds,” *Scientific Reports* **6** (2016), 10.1038/srep24372.
- ⁹L.-M. Zheng, J. Tang, H.-L. Sun, and M. Ren, “Low dimensional molecular magnets and spintronics,” in *Handbook of Spintronics*, edited by Y. Xu, D. D. Awschalom, and J. Nitta (Springer Netherlands, Dordrecht, 2016) pp. 617–680.
- ¹⁰A. E. Thorarinsdottir and T. D. Harris, “Metal–organic framework magnets,” *Chemical Reviews* **120**, 8716–8789 (2020), pMID: 32045215, <https://doi.org/10.1021/acs.chemrev.9b00666>.

- ¹¹M. Kurmoo, “Magnetic metal–organic frameworks,” *Chem. Soc. Rev.* **38**, 1353–1379 (2009).
- ¹²W. W. Lapo Bogani, “Molecular spintronics using single-molecule magnets,” *Nature Materials* **7**, 179–186 (2008).
- ¹³J. Gómez-Segura, J. Veciana, and D. Ruiz-Molina, “Advances on the nanostructuring of magnetic molecules on surfaces: the case of single-molecule magnets (smm),” *Chem. Commun.* , 3699–3707 (2007).
- ¹⁴G. Mínguez Espallargas and E. Coronado, “Magnetic functionalities in mofs: from the framework to the pore,” *Chem. Soc. Rev.* **47**, 533–557 (2018).
- ¹⁵J. M. Frost, K. L. M. Harriman, and M. Murugesu, “The rise of 3-d single-ion magnets in molecular magnetism: towards materials from molecules?” *Chem. Sci.* **7**, 2470–2491 (2016).
- ¹⁶K. Ziemelis, “The difficult middle ground,” *Nature Physics* **4**, S19 (2008).
- ¹⁷R. F. Weinland and G. Fischer, “Über manganiacetate und -benzoate,” *Zeitschrift für anorganische und allgemeine Chemie* **120**, 161–180 (1921), <https://onlinelibrary.wiley.com/doi/pdf/10.1002/zaac.19211200116>.
- ¹⁸T. Lis, “Preparation, structure, and magnetic properties of a dodecanuclear mixed-valence manganese carboxylate,” *Acta Crystallographica Section B* **36**, 2042–2046 (1980), <https://onlinelibrary.wiley.com/doi/pdf/10.1107/S0567740880007893>.
- ¹⁹P. D. W. Boyd, Q. Li, J. B. Vincent, K. Folting, H. R. Chang, W. E. Streib, J. C. Huffman, G. Christou, and D. N. Hendrickson, “Potential building blocks for molecular ferromagnets: $[\text{mn}_{12}\text{o}_{12}(\text{o}2\text{cph})_{16}(\text{h}2\text{o})_4]$ with a $s = 14$ ground state,” *Journal of the American Chemical Society* **110**, 8537–8539 (1988), <https://doi.org/10.1021/ja00233a036>.
- ²⁰A. Caneschi, D. Gatteschi, R. Sessoli, A. L. Barra, L. C. Brunel, and M. Guillot, “Alternating current susceptibility, high field magnetization, and millimeter band epr evidence for a ground $s = 10$ state in $[\text{mn}_{12}\text{o}_{12}(\text{ch}3\text{coo})_{16}(\text{h}2\text{o})_4].2\text{ch}3\text{cooh}.4\text{h}2\text{o}$,” *Journal of the American Chemical Society* **113**, 5873–5874 (1991), <https://doi.org/10.1021/ja00015a057>.
- ²¹R. Sessoli, H. L. Tsai, A. R. Schake, S. Wang, J. B. Vincent, K. Folting, D. Gatteschi, G. Christou, and D. N. Hendrickson, “High-spin molecules: $[\text{mn}_{12}\text{o}_{12}(\text{o}2\text{cr})_{16}(\text{h}2\text{o})_4]$,” *Journal of the American Chemical Society* **115**, 1804–1816 (1993), <https://doi.org/10.1021/ja00058a027>.
- ²²E. Cremades, J. Cano, E. Ruiz, G. Rajaraman, C. J. Milios, and E. K. Brechin,

- “Theoretical methods enlighten magnetic properties of a family of mn6 single-molecule magnets,” *Inorganic Chemistry* **48**, 8012–8019 (2009), pMID: 19624160, <https://doi.org/10.1021/ic900992r>.
- ²³E. Ruiz, T. Cauchy, J. Cano, R. Costa, J. Tercero, and S. Alvarez, “Magnetic structure of the large-spin mn10 and mn19 complexes: A theoretical complement to an experimental milestone,” *Journal of the American Chemical Society* **130**, 7420–7426 (2008), pMID: 18489093, <https://doi.org/10.1021/ja800092s>.
- ²⁴O. Waldmann, A. M. Ako, H. U. Güdel, and A. K. Powell, “Assessment of the anisotropy in the molecule mn19 with a high-spin ground state $s = 83/2$ by 35 ghz electron paramagnetic resonance,” *Inorganic Chemistry* **47**, 3486–3488 (2008), pMID: 18393411, <https://doi.org/10.1021/ic800213w>.
- ²⁵E. E. Moushi, T. C. Stamatatos, W. Wernsdorfer, V. Nastopoulos, G. Christou, and A. J. Tasiopoulos, “A family of 3d coordination polymers composed of mn19 magnetic units,” *Angewandte Chemie International Edition* **45**, 7722–7725 (2006), <https://onlinelibrary.wiley.com/doi/pdf/10.1002/anie.200603498>.
- ²⁶M. Murugesu, S. Takahashi, A. Wilson, K. A. Abboud, W. Wernsdorfer, S. Hill, and G. Christou, “Large mn25 single-molecule magnet with spin $s = 51/2$: Magnetic and high-frequency electron paramagnetic resonance spectroscopic characterization of a giant spin state,” *Inorganic Chemistry* **47**, 9459–9470 (2008), pMID: 18788733, <https://doi.org/10.1021/ic801142p>.
- ²⁷M. Murugesu, M. Habrych, W. Wernsdorfer, K. A. Abboud, and G. Christou, “Single-molecule magnets: A mn25 complex with a record $s = 51/2$ spin for a molecular species,” *Journal of the American Chemical Society* **126**, 4766–4767 (2004), pMID: 15080666, <https://doi.org/10.1021/ja0316824>.
- ²⁸P. Abbasi, K. Quinn, D. I. Alexandropoulos, M. Damjanović, W. Wernsdorfer, A. Escuer, J. Mayans, M. Pilkington, and T. C. Stamatatos, “Transition metal single-molecule magnets: A Mn31 nanosized cluster with a large energy barrier of 60 k and magnetic hysteresis at 5 k,” *Journal of the American Chemical Society* **139**, 15644–15647 (2017), pMID: 29052991, <https://doi.org/10.1021/jacs.7b10130>.
- ²⁹A. J. Tasiopoulos, A. Vinslava, W. Wernsdorfer, K. A. Abboud, and G. Christou, “Giant single-molecule magnets: A Mn84 torus and its supramolecular nanotubes,” *Angewandte Chemie International Edition* **43**, 2117–2121 (2004),

<https://onlinelibrary.wiley.com/doi/pdf/10.1002/anie.200353352>.

- ³⁰R. Hernández Sánchez and T. A. Betley, “Meta-atom behavior in clusters revealing large spin ground states,” *Journal of the American Chemical Society* **137**, 13949–13956 (2015), pMID: 26440452, <https://doi.org/10.1021/jacs.5b08962>.
- ³¹C. Sangregorio, T. Ohm, C. Paulsen, R. Sessoli, and D. Gatteschi, “Quantum tunneling of the magnetization in an iron cluster nanomagnet,” *Phys. Rev. Lett.* **78**, 4645–4648 (1997).
- ³²A. K. Powell, S. L. Heath, D. Gatteschi, L. Pardi, R. Sessoli, G. Spina, F. Del Giallo, and F. Pieralli, “Synthesis, structures, and magnetic properties of fe₂, fe₁₇, and fe₁₉ oxo-bridged iron clusters: The stabilization of high ground state spins by cluster aggregates,” *Journal of the American Chemical Society* **117**, 2491–2502 (1995), <https://doi.org/10.1021/ja00114a012>.
- ³³C. Cadiou, M. Murrie, C. Paulsen, V. Villar, W. Wernsdorfer, and R. E. P. Winpenny, “Studies of a nickel-based single molecule magnet: resonant quantum tunnelling in an $s = 12$ molecule,” *Chem. Commun.* , 2666–2667 (2001).
- ³⁴M. Murrie, S. J. Teat, H. Stöckli-Evans, and H. U. Güdel, “Synthesis and characterization of a cobalt(ii) single-molecule magnet,” *Angewandte Chemie International Edition* **42**, 4653–4656 (2003), <https://onlinelibrary.wiley.com/doi/pdf/10.1002/anie.200351753>.
- ³⁵Y.-Z. Zhang, W. Wernsdorfer, F. Pan, Z.-M. Wang, and S. Gao, “An azido-bridged disc-like heptanuclear cobalt(ii) cluster: towards a single-molecule magnet,” *Chem. Commun.* , 3302–3304 (2006).
- ³⁶A.-L. Barra, P. Debrunner, D. Gatteschi, C. E. Schulz, and R. Sessoli, “Superparamagnetic-like behavior in an octanuclear iron cluster,” *Europhysics Letters (EPL)* **35**, 133–138 (1996).
- ³⁷O. Waldmann, “A criterion for the anisotropy barrier in single-molecule magnets,” *Inorganic Chemistry* **46**, 10035–10037 (2007), pMID: 17979271, <https://doi.org/10.1021/ic701365t>.
- ³⁸F. Neese and D. A. Pantazis, “What is not required to make a single molecule magnet,” *Faraday Discuss.* **148**, 229–238 (2011).
- ³⁹H. Oshio and M. Nakano, “High-spin molecules with magnetic anisotropy toward single-molecule magnets,” *Chemistry – A European Journal* **11**, 5178–5185 (2005), <https://chemistry-europe.onlinelibrary.wiley.com/doi/pdf/10.1002/chem.200401100>.

- ⁴⁰E. Ruiz, J. Cirera, J. Cano, S. Alvarez, C. Loose, and J. Kortus, “Can large magnetic anisotropy and high spin really coexist?” *Chem. Commun.* , 52–54 (2008).
- ⁴¹L. M. C. Beltran and J. R. Long, “Directed assembly of metal-cyanide cluster magnets,” *Accounts of Chemical Research* **38**, 325–334 (2005), pMID: 15835879, <https://doi.org/10.1021/ar040158e>.
- ⁴²X.-Y. Wang, C. Avendaño, and K. R. Dunbar, “Molecular magnetic materials based on 4d and 5d transition metals,” *Chem. Soc. Rev.* **40**, 3213–3238 (2011).
- ⁴³K. S. Pedersen, J. Bendix, and R. Clérac, “Single-molecule magnet engineering: building-block approaches,” *Chem. Commun.* **50**, 4396–4415 (2014).
- ⁴⁴D. N. Woodruff, R. E. P. Winpenny, and R. A. Layfield, “Lanthanide single-molecule magnets,” *Chemical Reviews* **113**, 5110–5148 (2013), pMID: 23550940, <https://doi.org/10.1021/cr400018q>.
- ⁴⁵F.-S. Guo, A. K. Bar, and R. A. Layfield, “Main group chemistry at the interface with molecular magnetism,” *Chemical Reviews* **119**, 8479–8505 (2019), pMID: 31059235, <https://doi.org/10.1021/acs.chemrev.9b00103>.
- ⁴⁶R. Sessoli and A. K. Powell, “Strategies towards single molecule magnets based on lanthanide ions,” *Coordination Chemistry Reviews* **253**, 2328 – 2341 (2009), deutsche Forschungsgemeinschaft Molecular Magnetism Research Report.
- ⁴⁷S. G. McAdams, A.-M. Ariciu, A. K. Kostopoulos, J. P. Walsh, and F. Tuna, “Molecular single-ion magnets based on lanthanides and actinides: Design considerations and new advances in the context of quantum technologies,” *Coordination Chemistry Reviews* **346**, 216 – 239 (2017), sI: 42 iccc, Brest– by invitation.
- ⁴⁸Z. Zhu, M. Guo, X.-L. Li, and J. Tang, “Molecular magnetism of lanthanide: Advances and perspectives,” *Coordination Chemistry Reviews* **378**, 350 – 364 (2019), special issue on the 8th Chinese Coordination Chemistry Conference.
- ⁴⁹A. Dey, J. Acharya, and V. Chandrasekhar, “Heterometallic 3d–4f complexes as single-molecule magnets,” *Chemistry – An Asian Journal* **14**, 4433–4453 (2019).
- ⁵⁰S. Demir, I.-R. Jeon, J. R. Long, and T. D. Harris, “Radical ligand-containing single-molecule magnets,” *COORDINATION CHEMISTRY REVIEWS* **289**, 149–176 (2015).
- ⁵¹R. A. Layfield, “Organometallic single-molecule magnets,” *Organometallics* **33**, 1084–1099 (2014).
- ⁵²P. Hohenberg and W. Kohn, “Inhomogeneous electron gas,” *Physical review* **136**, B864

(1964).

- ⁵³R. G. Parr and R. G. P. W. Yang, *Density-functional theory of atoms and molecules* (Oxford university press, 1989).
- ⁵⁴R. Dreizler and E. Gross, *Density Functional Theory: An Approach to the Quantum Many-Body Problem* (Springer, 1990).
- ⁵⁵E. Engel and R. M. Dreizler, *Density functional theory* (Springer, 2013).
- ⁵⁶R. Barnett and U. Landman, Phys. Rev. B **48**, 2081 (1993).
- ⁵⁷D. Marx and J. Hutter, *Ab Initio Molecular Dynamics: Basic Theory and Advanced Methods* (Cambridge Univ. Press, Cambridge, 2009).
- ⁵⁸H. Schlosser and P. M. Marcus, “Composite wave variational method for solution of the energy-band problem in solids,” Physical Review **131**, 2529–2546 (1963).
- ⁵⁹D. Vanderbilt, “Soft self-consistent pseudopotentials in a generalized eigenvalue formalism,” Physical Review B **41**, 7892 (1990).
- ⁶⁰P. Blöchl, “Projector augmented-wave method,” Phys. Rev. B **50**, 17953–17979 (1994).
- ⁶¹G. Kresse and J. Furthmüller, “Efficient iterative schemes for ab initio total-energy calculations using a plane-wave basis set,” Phys. Rev. B **54**, 11169–11186 (1996).
- ⁶²P. Giannozzi, S. Baroni, N. Bonini, M. Calandra, R. Car, C. Cavazzoni, D. Ceresoli, G. L. Chiarotti, M. Cococcioni, I. Dabo, A. D. Corso, S. de Gironcoli, S. Fabris, G. Fratesi, R. Gebauer, U. Gerstmann, C. Gougoussis, A. Kokalj, M. Lazzeri, L. Martin-Samos, N. Marzari, F. Mauri, R. Mazzarello, S. Paolini, A. Pasquarello, L. Paulatto, C. Sbraccia, S. Scandolo, G. Sclauzero, A. P. Seitsonen, A. Smogunov, P. Umari, and R. M. Wentzcovitch, “Quantum espresso: a modular and open-source software project for quantum simulations of materials,” Journal of Physics: Condensed Matter **21**, 395502 (2009).
- ⁶³X. Gonze, B. Amadon, P.-M. Anglade, J.-M. Beuken, F. Bottin, P. Boulanger, F. Bruneval, D. Caliste, R. Caracas, M. Côté, T. Deutsch, L. Genovese, P. Ghosez, M. Giantomassi, S. Goedecker, D. Hamann, P. Hermet, F. Jollet, G. Jomard, S. Leroux, M. Mancini, S. Mazevet, M. Oliveira, G. Onida, Y. Pouillon, T. Rangel, G.-M. Rignanese, D. Sangalli, R. Shaltaf, M. Torrent, M. Verstraete, G. Zerah, and J. Zwanziger, “Abinit: First-principles approach to material and nanosystem properties,” Computer Physics Communications **180**, 2582–2615 (2009), 40 YEARS OF CPC: A celebratory issue focused on quality software for high performance, grid and novel computing architectures.

- ⁶⁴X. Gonze, J.-M. Beuken, R. Caracas, F. Detraux, M. Fuchs, G.-M. Rignanese, L. Sindic, M. Verstraete, G. Zerah, F. Jollet, M. Torrent, A. Roy, M. Mikami, P. Ghosez, J.-Y. Raty, and D. Allan, “First-principles computation of material properties: the abinit software project,” *Computational Materials Science* **25**, 478 – 492 (2002).
- ⁶⁵M. Torrent, F. Jollet, F. Bottin, G. Zerah, and X. Gonze, “Implementation of the projector augmented-wave method in the abinit code: Application to the study of iron under pressure,” *Computational Materials Science* **42**, 337 – 351 (2008).
- ⁶⁶J. Paier, M. Marsman, K. Hummer, G. Kresse, I. C. Gerber, and J. G.Ángyán, “Screened hybrid density functionals applied to solids,” *Journal of Chemical Physics* **124**, 154709 (2006).
- ⁶⁷P. Haas, F. Tran, and P. Blaha, “Calculation of the lattice constant of solids with semilocal functionals,” *Physical Review B* **79**, 085104 (2009).
- ⁶⁸Y. Fu and D. Singh, “Applicability of the strongly constrained and appropriately normed density functional to transition-metal magnetism,” *Physical Review Letters* **121**, 207201 (2018).
- ⁶⁹D. J. Singh and L. Nordstrom, *Plane Waves, Pseudopotentials, and the LAPW Method*, 2nd ed. (Springer, 2006).
- ⁷⁰J. Slater, “Wave functions in a periodic potential,” *Physical Review* **51**, 846–851 (1937).
- ⁷¹J. Slater, “An augmented plane wave method for the periodic potential problem,” *Physical Review* **92**, 603–608 (1953).
- ⁷²R. S. Leigh, “The augmented plane wave and related methods for crystal eigenvalue problems,” *Proceedings of the Physical Society A* **69**, 388–400 (1956).
- ⁷³T. Loucks, *The Augmented Plane Wave Method* (Benjamin, New York, 1967).
- ⁷⁴J. Slater, “Xxx,” in *Methods of Computational Physics*, Vol. 8, edited by B. Alder, S. Fernbach, and M. Rotenberg (Academic, New York, 1968) pp. 1–XX.
- ⁷⁵L. Mattheiss, A. Switendick, and J. Wood, “Xxx,” in *Methods of Computational Physics*, Vol. 8, edited by B. Alder, S. Fernbach, and M. Rotenberg (Academic, New York, 1968) pp. 899–XX.
- ⁷⁶P. Marcus, “Variational methods in the computation of energy bands,” *International Journal of Quantum Chemistry Symposium* **1**, 567–XXX (1967).
- ⁷⁷D. Koelling, “Linearized form of the apw method,” *Journal of Physics and Chemistry of Solids* **33**, 1335–1338 (1972).

- ⁷⁸O. Andersen, “Simple approach to the band-structure problem,” *Solid State Communications* **13**, 133–136 (1973).
- ⁷⁹O. Andersen, “Linear methods in band theory,” *Physical Review B* **12**, 3060–3083 (1975).
- ⁸⁰D. Koelling and G. Arbman, “Use of energy derivative of the radial solution in an augmented plane wave method: application to copper,” *Journal of Physics F* **5**, 2041–2054 (1975).
- ⁸¹D. Koelling and B. Harmon, “[] a technique for relativistic spin-polarised calculations,” *Journal of Physics C* **10**, 3107–3114 (1977).
- ⁸²E. Wimmer, H. Krakauer, M. Weinert, and A. Freeman, “Full-potential self-consistent linearized-augmented-plane-wave method for calculating the electronic structure of molecules and surfaces: O₂ molecule,” *Physical Review B* **24**, 864–875 (1981).
- ⁸³M. Weinert, “Solution of poisson’s equation: Beyond ewald-type methods,” *Journal of Mathematical Physics* **22**, 2433–2439 (1981).
- ⁸⁴M. Weinert, E. Wimmer, and A. Freeman, “Total-energy all-electron density functional method for bulk solids and surfaces,” *Physical Review B* **26**, 4571–4578 (1982).
- ⁸⁵P. Blaha and K. Schwarz, “Electron densities and chemical bonding in tic, tin, and tio derived from energy band calculations,” *International Journal of Quantum Chemistry* **XXIII**, 1535–1552 (1983).
- ⁸⁶H. Jansen and A. Freeman, “Total-energy full-potential linearized augmented-plane-wave method for bulk solids: Electronic and structural properties of tungsten,” *Physical Review B* **30**, 561–569 (1984).
- ⁸⁷P. Blaha, K. Schwarz, and P. Herzig, “First-principles calculation of the electric field gradient of li₃n,” *Physical Review Letters* **54**, 1192–1195 (1985).
- ⁸⁸S. Wei, H. Krakauer, and M. Weinert, “Linearized augmented-plane-wave calculation of the electronic structure and total energy of tungsten,” *Physical Review B* **32**, 7792–7797 (1985).
- ⁸⁹L. Mattheiss and D. Hamann, “Linear augmented-plane-wave calculation of the structural properties of bulk cr, mo, and w,” *Physical Review B* **33**, 823–840 (1986).
- ⁹⁰S. Goedecker and K. Maschke, “Operator approach in the linearized augmented-plane-wave method: Efficient electronic-structure calculations including forces,” *Physical Review B* **45**, 1597–1604 (1992).
- ⁹¹D. J. Singh, “Ground-state properties of lanthanum: Treatment of extended-core states,”

- Physical Review B **43**, 6388–6392 (1991).
- ⁹²E. Sjöstedt, L. Nordstrom, and D. Singh, “An alternative way of linearizing the augmented plane-wave method,” *Solid State Communications* **114**, 15–20 (2000).
- ⁹³S. Cottenier, *Density Functional Theory and the Family of (L)APW-methods: a step-by-step introduction* (self-published, 2013) ISBN 978-90-807215-1-7.
- ⁹⁴P. Blaha, K. Schwarz, and S. Trickey, “Electronic structure of solids with wien2k,” *Molecular Physics* **108**, 3147–3166 (2010).
- ⁹⁵K. Schwarz, “Computation of materials properties at atomic scale,” in *Selected Topics in Applications of Quantum Mechanics*, edited by M. R. Pahlavani (IntechOpen, London, 2015) pp. 275–310.
- ⁹⁶A. Gulans, S. Kontur, C. Meisenbichler, D. Nabok, P. Pavone, S. Rigamonti, S. Sagmeister, U. Werner, and C. Draxl, “exciting — a full-potential all-electron package implementing density-functional theory and many-body perturbation theory,” *Journal of Physics: Condensed Matter* **26**, 363202 (2014).
- ⁹⁷R. Solcá, A. Kozhevnikov, A. Haidar, S. Tomov, J. Dongarra, and T. C. Schulthess, “Efficient implementation of quantum materials simulations on distributed cpu-gpu systems,” in *Proceedings of the International Conference for High Performance Computing, Networking, Storage and Analysis, ser. SC '15* (ACM, New York, NY, 2015) p. 1–12.
- ⁹⁸P. Blaha, K. Schwarz, P. Sorantin, and S. Trickey, “Full-potential, linearized augmented plane wave programs for crystalline systems,” *Computer Physics Communications* **59**, 399–415 (1990).
- ⁹⁹P. Blaha, K. Schwarz, F. Tran, R. Laskowski, G. Madsen, and L. Marks, “Wien2k: An apw+lo program for calculating the properties of solids,” *Journal of Chemical Physics* **152**, 074101 (2020).
- ¹⁰⁰“The Elk Code,” <http://elk.sourceforge.net>.
- ¹⁰¹“The Fleur Code,” <http://www.flapw.de>.
- ¹⁰²A. Kozhevnikov, A. G. Eguluz, and T. C. Schulthess, “Toward first principles electronic structure simulations of excited states and strong correlations in nano- and materials science,” 2010 ACM/IEEE International Conference for High Performance Computing, Networking, Storage and Analysis , 1–10 (2010).
- ¹⁰³M. Petersilka, U. J. Gossmann, and E. K. U. Gross, “Excitation energies from time-dependent density-functional theory,” *Phys. Rev. Lett.* **76**, 1212–1215 (1996).

- ¹⁰⁴I.-H. Chu, J. P. Trinastic, Y.-P. Wang, A. G. Eguiluz, A. Kozhevnikov, T. C. Schulthess, and H.-P. Cheng, “All-electron self-consistent gw in the matsubara-time domain: Implementation and benchmarks of semiconductors and insulators,” *Phys. Rev. B* **93**, 125210 (2016).
- ¹⁰⁵E. Anderson, Z. Bai, C. Bischof, S. Blackford, J. Demmel, J. Dongarra, J. Du Croz, A. Greenbaum, S. Hammarling, A. McKenney, and D. Sorensen, *LAPACK Users’ Guide*, 3rd ed. (Society for Industrial and Applied Mathematics, Philadelphia, PA, 1999).
- ¹⁰⁶“Cuda toolkit documentation,” <https://docs.nvidia.com/cuda/index.html> (), version: v11.2.1.
- ¹⁰⁷N. M. Josuttis, *The C++ Standard Library: A Tutorial and Reference*, 3rd ed. (Addison-Wesley, Philadelphia, PA, 2000).
- ¹⁰⁸“Nvcc compiler,” <https://docs.nvidia.com/cuda/cuda-compiler-driver-nvcc/> ().
- ¹⁰⁹P. Blaha, H. Hofstätter, O. Koch, R. Laskowski, and K. Schwarz, “Iterative diagonalization in augmented plane wave based methods in electronic structure calculations,” *Journal of Computational Physics* **229**, 453–460 (2010).
- ¹¹⁰A. Gulans, “Implementation of davidson iterative eigen solver for lapw,” to be published.
- ¹¹¹P. G. Sim and E. Sinn, “First manganese(iii) spin crossover, first d4 crossover. comment on cytochrome oxidase,” *Journal of the American Chemical Society* **103**, 241–243 (1981), <https://doi.org/10.1021/ja00391a067>.
- ¹¹²V. S. Zapf, D. Zocco, B. R. Hansen, M. Jaime, N. Harrison, C. D. Batista, M. Kenzelmann, C. Niedermayer, A. Lacerda, and A. Paduan-Filho, “Bose-einstein condensation of $s = 1$ nickel spin degrees of freedom in $\text{NiCl}_2-4\text{SC}(\text{NH}_2)_2$,” *Phys. Rev. Lett.* **96**, 077204 (2006).
- ¹¹³S. A. Zvyagin, J. Wosnitza, C. D. Batista, M. Tsukamoto, N. Kawashima, J. Krzystek, V. S. Zapf, M. Jaime, N. F. Oliveira, and A. Paduan-Filho, “Magnetic excitations in the spin-1 anisotropic heisenberg antiferromagnetic chain system $\text{NiCl}_2-4\text{SC}(\text{NH}_2)_2$,” *Phys. Rev. Lett.* **98**, 047205 (2007).
- ¹¹⁴V. S. Zapf, P. Sengupta, C. D. Batista, F. Nasreen, F. Wolff-Fabris, and A. Paduan-Filho, “Magnetoelectric effects in an organometallic quantum magnet,” *Phys. Rev. B* **83**, 140405 (2011).
- ¹¹⁵V. S. Zapf, V. F. Correa, P. Sengupta, C. D. Batista, M. Tsukamoto, N. Kawashima, P. Egan, C. Pantea, A. Migliori, J. B. Betts, M. Jaime, and A. Paduan-Filho, “Direct measurement of spin correlations using magnetostriction,” *Phys. Rev. B* **77**, 020404 (2008).

- ¹¹⁶M. Yazback, J.-X. Yu, S. Liu, L. Zhang, N. S. Sullivan, and H.-P. Cheng, “First-principles study of an $s = 1$ quasi one-dimensional quantum molecular magnetic material,” *Phys. Rev. B* **103**, 054434 (2021).
- ¹¹⁷S. Hill, R. S. Edwards, N. Aliaga-Alcalde, and G. Christou, “Quantum coherence in an exchange-coupled dimer of single-molecule magnets,” *Science* **302**, 1015–1018 (2003), <https://science.sciencemag.org/content/302/5647/1015.full.pdf>.
- ¹¹⁸A. Wilson, S. Hill, R. S. Edwards, N. Aliaga-Alcalde, and G. Christou, “Entanglement of exchange-coupled dimers of single-molecule magnets,” *AIP Conference Proceedings* **850**, 1141–1142 (2006), <https://aip.scitation.org/doi/pdf/10.1063/1.2355106>.
- ¹¹⁹R. Tiron, W. Wernsdorfer, D. Foguet-Albiol, N. Aliaga-Alcalde, and G. Christou, “Spin quantum tunneling via entangled states in a dimer of exchange-coupled single-molecule magnets,” *Phys. Rev. Lett.* **91**, 227203 (2003).
- ¹²⁰T. N. Nguyen, W. Wernsdorfer, K. A. Abboud, and G. Christou, “A supramolecular aggregate of four exchange-biased single-molecule magnets,” *Journal of the American Chemical Society* **133**, 20688–20691 (2011), pMID: 22136491, <https://doi.org/10.1021/ja2087344>.
- ¹²¹T. N. Nguyen, M. Shiddiq, T. Ghosh, K. A. Abboud, S. Hill, and G. Christou, “Covalently linked dimer of mn3 single-molecule magnets and retention of its structure and quantum properties in solution,” *Journal of the American Chemical Society* **137**, 7160–7168 (2015), pMID: 26027646, <https://doi.org/10.1021/jacs.5b02677>.